Vacuum 149 (2018) 106–113

Contents lists available at ScienceDirect

Vacuum

journal homepage: www.elsevier.com/locate/vacuum

Effects of pre-aging and minor Sc addition on the microstructure and mechanical properties of friction stir processed 7055 Al alloy

C.Y. Liu [a, b, *], B. Zhang [c], Z.Y. Ma [b, **], G.B. Teng [a], L.L. Wei [a], W.B. Zhou [d], X.Y. Zhang [c]

[a] Key Laboratory of New Processing Technology for Nonferrous Metal & Materials, Ministry of Education, Guilin University of Technology, Guilin 541004, China
[b] Shenyang National Laboratory for Materials Science, Institute of Metal Research, Chinese Academy of Sciences, 72 Wenhua Road, Shenyang 110016, China
[c] State Key Laboratory of Metastable Materials Science and Technology, Yanshan University, Qinhuangdao 066004, China
[d] Alnan Aluminium Co., Ltd., Nanning 530000, China

ARTICLE INFO

Article history:
Received 2 December 2017
Received in revised form
18 December 2017
Accepted 19 December 2017
Available online 20 December 2017

Keywords:
Al alloy
Friction stir processing
Microstructure
Mechanical properties

ABSTRACT

The effects of Sc addition and pre-aging on the microstructure and mechanical properties of friction stir processed (FSP) 7055 Al alloy were investigated. The addition of Sc effectively inhibited the coarsening of grains in the FSP 7055 Al alloy due to the grain boundary pinning effect of $Al_3(Sc,Zr)$ particles. The high density of $Al_3(Sc,Zr)$ particles also provided more preferential nucleation sites for the precipitation of the η phase during FSP, and then inhibited the coarsening and increased the density of the η phase in the FSP 7055 alloy. The η′ phase precipitated in the 7055 and Sc-containing 7055 during artificial aging, and then dissolved into the Al matrix during FSP. Thus, pre-aging effectively inhibited the formation of the η phase during FSP, and increased the quantity of the solute atoms in the FSP samples. The mechanical properties of the FSP 7055 Al alloy were improved by the addition of Sc and pre-aging. The aged 7055–0.25Sc Al alloy with FSP showed the highest ultimate tensile strength of 578 MPa; and the aged 7055 Al alloy with FSP showed the largest elongation of 21%. This work provides an effective strategy to improve the mechanical properties of FSP Al alloys.

1. Introduction

Al alloys with ultra-fine-grained (UFG) structure have attracted wide attention due to their excellent physical and mechanical properties [1–4]. In the past few years, friction stir processing (FSP), which was developed based on the basic principles of friction stir welding (FSW) [5,6] has been used to fabricate UFG Al alloys, due to its simplicity, effectiveness and variability in grain refinement [7–10].

Al-Zn-Mg(-Cu) series (7xxx) alloys have been widely used in the aeronautics and astronautics industries due to their low density, ultra-high strength and fracture toughness [11–15]. UFG 7xxx Al alloys have also been successfully fabricated by FSP [16–20], and it has been found that the FSP 7xxx Al alloys exhibit superplasticity when the deformation temperature is higher than 200 °C. However, the investigation into the room-temperature mechanical properties of the FSP 7xxx Al alloys is limited so far.

Softening in the stir zone (SZ) has been widely reported in the 7xxx Al alloys during FSW [21–29]. The 7xxx Al alloys are typical aging-hardened alloys, and precipitation occurs in these alloys during FSW or FSP owing to the friction-induced temperature rise. The structure, size, density and distribution of the precipitated phases strongly affect the room-temperature mechanical properties of the FSP 7xxx Al alloys, such as the tensile strength and ductility. Clearly, controlling the precipitation process is the key to producing FSP 7xxx Al alloys with excellent room-temperature mechanical properties.

The precipitation sequence of 7xxx Al alloys is described as: supersaturated solid solution → GP zones → metastable η′ phase → stable η phase [30]. The high density of the η phase, which corresponds to the over-aging state of the 7xxx Al alloys, has always been obtained in the SZ of FSW or FSP 7xxx Al alloys due to the large heat input [19,21], resulting in reduced strength of these FSP/FSW samples. Chen et al. [21] and Sharma et al. [25] found that applying the aging treatment before FSP/FSW can affect the precipitation process of the Al-6Zn-2.2Mg-1.6Cu (7B04) and Al-4.7Zn-2.4Mg-0.7Mn (7039) alloys during FSP/FSW, and therefore enhance the hardness of the SZ. This implies that the room-temperature

* Corresponding author. Key Laboratory of New Processing Technology for Nonferrous Metal & Materials, Ministry of Education, Guilin University of Technology, Guilin 541004, China. Tel.: +86 773 5896436.
** Corresponding author. Tel.: +86 24 83978908.
E-mail addresses: lcy261@glut.edu.cn (C.Y. Liu), zyma@imr.ac.cn (Z.Y. Ma).

https://doi.org/10.1016/j.vacuum.2017.12.030
0042-207X/

Table 1
Chemical composition of the 7055 and 7055–0.25Sc alloys.

	Zn	Mg	Cu	Zr	Sc
7055	7.82	1.95	2.24	0.16	–
7055–0.25Sc	7.81	1.93	2.24	0.16	0.25

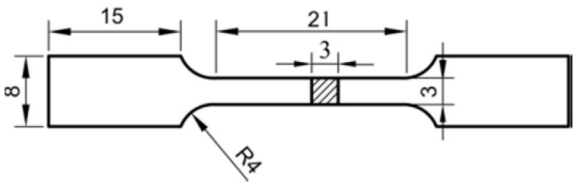

Fig. 1. Schematic drawing of the tensile specimen (mm).

mechanical properties of the FSP 7xxx Al alloys can be improved by optimizing the pre-aging.

The room-temperature mechanical properties of the FSP 7xxx Al alloys are also affected by the grain size. A low rotation rate is effective in reducing heat input during FSP/FSW [30–33], and can therefore can inhibit grain coarsening and enhance the strength of FSP/FSW samples. Furthermore, Deng et al. [29] found that the addition of Sc can also refine the grains of the SZ in the FSW joints of 7xxx Al alloys. The addition of Sc has been proven to be an effective approach in refining the grains of several Al alloys during heat treatment or deformation [34–37]. Thus, the room-temperature mechanical properties of the FSP 7xxx Al alloys are expected to improve through both a low rotation rate and the addition of Sc.

In the present study, an 7055 Al alloy was used as a raw material to investigate the effects of pre-aging and Sc addition on the microstructure and mechanical properties of the FSP 7xxx Al alloys with a low rotation rate (300 rpm). The aim is to fabricate UFG 7xxx Al alloys with excellent room-temperature mechanical properties.

2. Experimental methods

3 mm thick rolled sheets of 7055 Al alloy and 7055 Al alloy containing 0.25% (mass ratio) Sc (7055–0.25Sc) were used as raw materials. The chemical compositions of these two alloys are shown in Table 1. The sheets were subjected to a solution treatment in a vacuum furnace at 470 °C for 2 h, and then water quenched (defined as SS). Some of the SS 7055 and 7055–0.25Sc samples were aged at 120 °C for 12 h.

Both the SS and aged samples were subjected to FSP at a constant traverse speed of 100 mm min^{-1} with a low tool rotation rate of 300 rpm. A tool with a concave shoulder 10 mm in diameter and a taper threaded pin 2.7 mm in length and 5 mm in diameter was used.

The microstructures of the samples were examined using optical microscopy (OM), electron backscattered diffraction (EBSD) and transmission electron microscopy (TEM, JEM-2010). EBSD measurements were carried out using a Hitachi S-3400N-II scanning electron microscope. The films were prepared for TEM by grinding to a thickness of 50 μm, followed by thinning using a twinjet electropolishing device. Differential scanning calorimetry (DSC) was used to examine the transition temperature of the samples at a heating rate of 10 °C/min.

The tensile tests were conducted on an Instron-3369-type testing machine at a strain rate of 4×10^{-4} s^{-1}. The specimens for tensile testing were machined parallel to the FSP direction. Fig. 1 shows the dimension and shape of the tensile specimen. The fracture surfaces following the tensile tests were observed using scanning electron microscopy (S-4800).

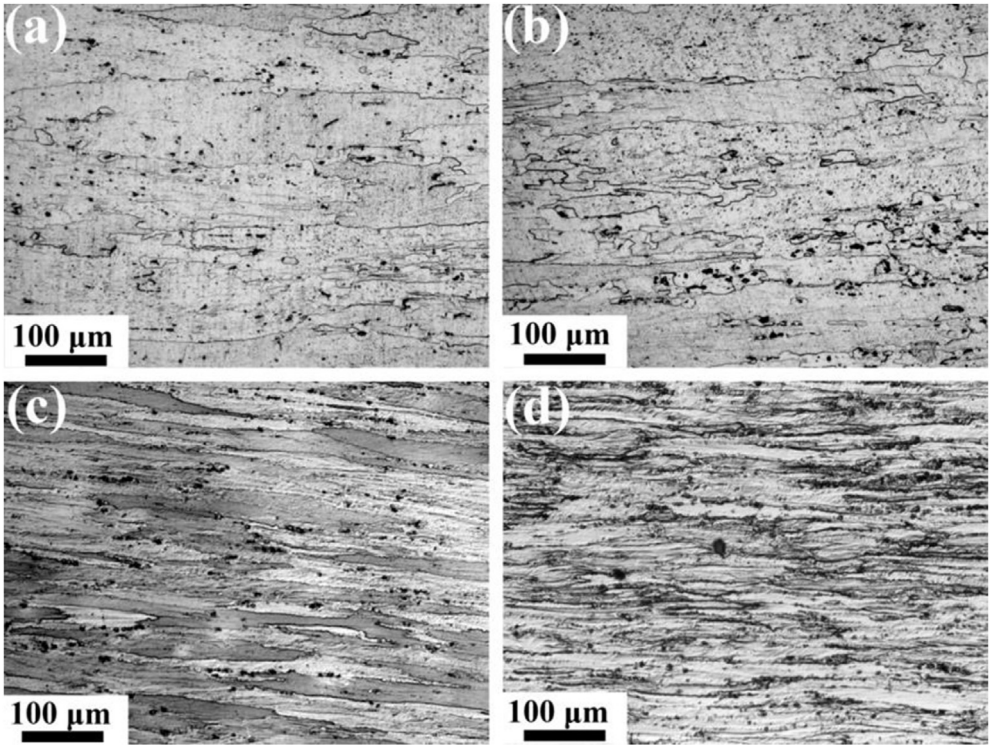

Fig. 2. OM micrographs of (a) SS and (b) aged 7055 samples, and (c) SS and (d) aged 7055–0.25Sc samples.

3. Results

Fig. 2 shows the OM micrographs of the SS and aged samples. The grain sizes of the 7055–0.25Sc samples were significantly smaller than those of the 7055 samples under the same heat treatment process. Recrystallized grains were observed in the SS and aged 7055 samples (Fig. 2a and b). However, no recrystallization grains were observed for the 7055–0.25Sc alloy sheets after solution and aging, and the fibrous rolling deformation structure was well preserved (Fig. 2c and d).

Fig. 3 shows TEM micrographs of the SS and aged samples. Equiaxed particles with sizes of 20–30 nm were observed in the SS 7055 sample (Fig. 3a). According to the chemical composition and heat treatment process, these particles should represent the Al_3Zr phase [38]. For the aged 7055 sample, a high density of η′ precipitates was observed in the grain interior, and η precipitates with larger sizes were discontinuously distributed along the GBs (Fig. 3b).

When added to Al alloys containing Zr, Sc can partially substitute for Zr, forming coherent $Al_3(Sc,Zr)$ precipitates during homogenizing and solution treatments [39]. Thus, a high density of nano-sized $Al_3(Sc,Zr)$ particles were observed in the SS 7055–0.25Sc sample (Fig. 3c). In the aged 7055–0.25Sc sample, η′ precipitates were observed in the grain and $Al_3(Sc,Zr)$ particles at the dislocations and GBs (Fig. 3d).

Figs. 4 and 5 show the microstructures and grain size distributions, respectively, of the FSP alloys obtained by EBSD. Completely recrystallized grains with equiaxed shape were observed in all the FSP samples. The FSP SS 7055 sample exhibited a multi-scale grain structure composed of fine grains (as small as 0.5 μm) and coarse grains (larger than 20 μm). The average grain size of this sample was ~3.6 μm (Figs. 4a and 5a). Pre-aging led to coarsening and a more uniform distribution of the recrystallized grains in the FSP 7055 sample, and the average grain size of the FSP aged 7055 sample was determined to be ~4.7 μm (Figs. 4b and 5b).

The FSP SS 7055–0.25Sc sample also exhibited a multi-scale grain structure, but the proportion of large grains in this sample was lower than that in the FSP SS 7055 sample. The average grain size of the FSP SS 7055–0.25Sc sample was ~1.7 μm (Figs. 4c and 5c). Pre-aging also led to the coarsening of the recrystallized grains in the FSP 7055–0.25Sc sample, and the average grain size increased to ~2.2 μm, which was much smaller than that of the FSP aged 7055 sample (Figs. 4d and 5d).

Fig. 6 shows the TEM micrographs of the FSP samples. A precipitated η phase with size larger than 100 nm was observed in all the FSP samples. Al_3Zr particles were observed in the precipitated η phase in the FSP SS 7055 sample (Fig. 6a). Compared with the FSP SS 7055 sample, the FSP aged 7055 sample exhibited a larger size and lower density of the η phase (Fig. 6b).

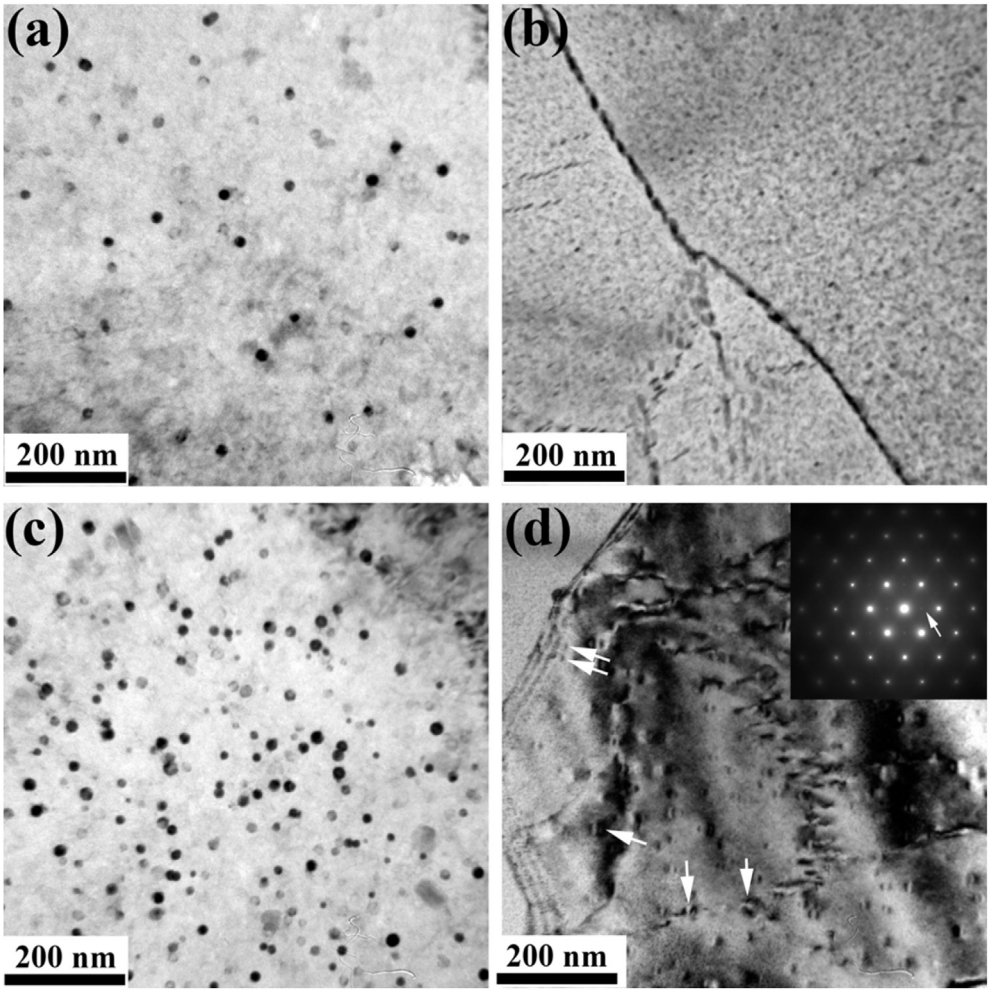

Fig. 3. TEM micrographs of (a) SS and (b) aged 7055 samples, and (c) SS and (d) aged 7055–0.25Sc samples. The arrows in (d) indicate the $Al_3(Sc,Zr)$ phase located at the dislocations and GBs.

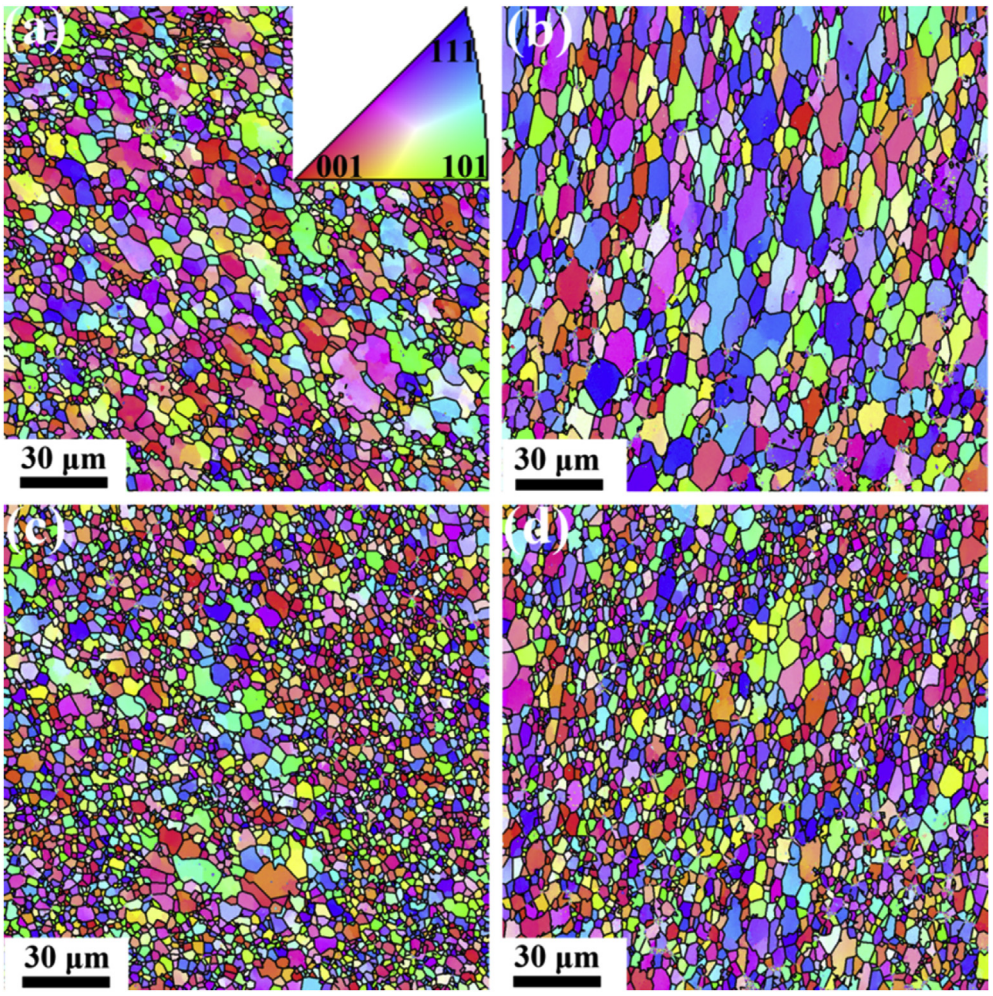

Fig. 4. EBSD maps showing the grain structure of FSP (a) SS and (b) aged 7055 samples, and (c) SS and (d) aged 7055−0.25Sc samples.

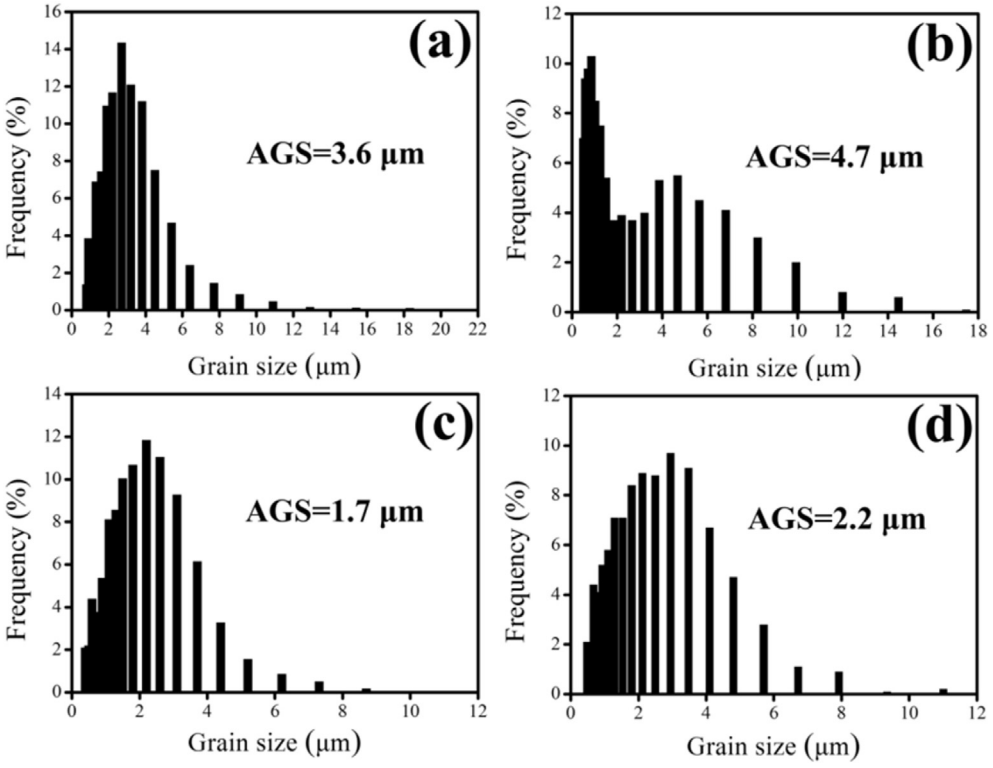

Fig. 5. Grain size distributions of FSP (a) SS and (b) aged 7055 samples, and (c) SS and (d) aged 7055−0.25Sc samples.

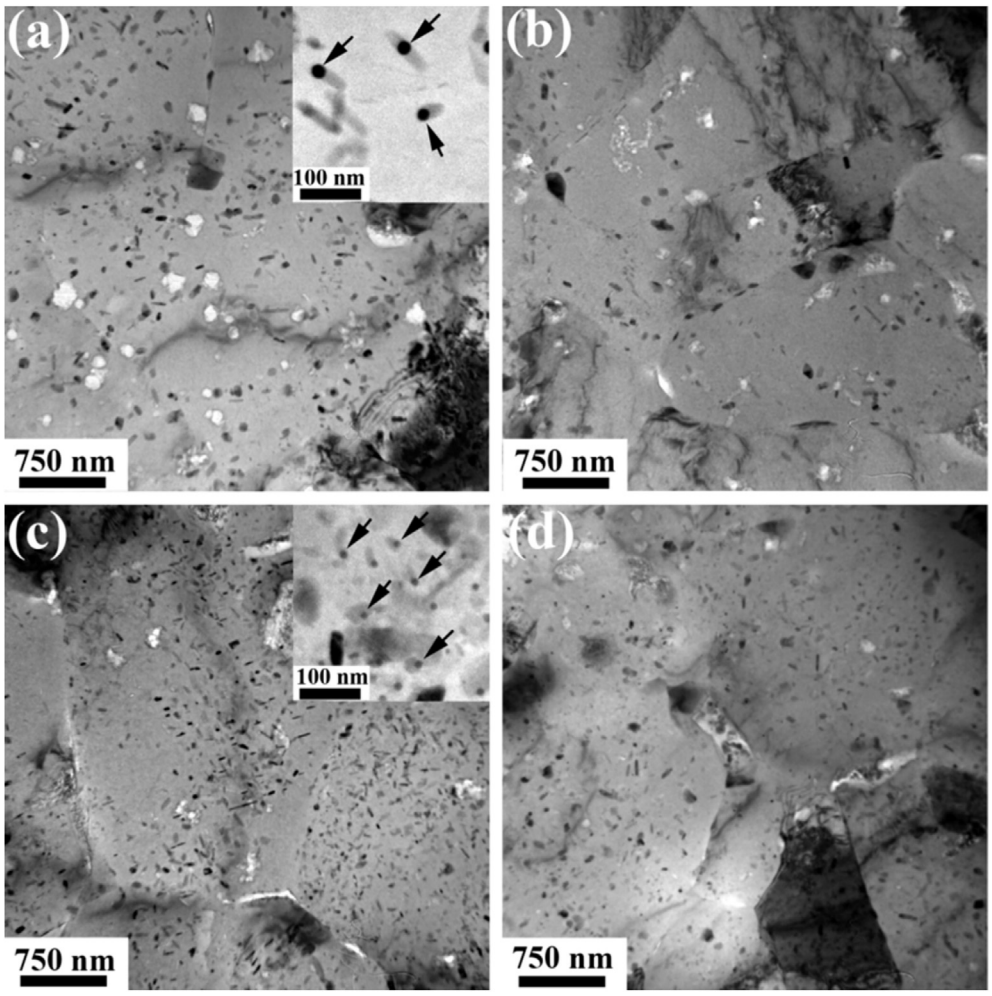

Fig. 6. TEM micrographs of FSP (a) SS and (b) aged 7055 samples, and (c) SS and (d) aged 7055–0.25Sc samples.

The addition of Sc reduced the size and increased the density of the η phase in the FSP SS samples. $Al_3(Zr,Sc)$ particles were also observed in the η phase in the FSP SS 7055–0.25Sc sample (Fig. 6c). The FSP aged 7055–0.25Sc sample exhibited a larger size and lower density of the η phase compared to the FSP SS 7055–0.25Sc sample (Fig. 6d).

Fig. 7 shows the DSC curves for the 7055–0.25Sc samples under various conditions. Peak A, which was related to the dissolution of GP zones [23], was observed in the SS and FSP samples, and the FSP SS sample exhibited a lower intensity of peak A than the SS and FSP aged samples. Peak B, which was related to the dissolution of the η′ phase [23], was only observed in the aged sample. A peak in the η phase precipitation (peak C) was obtained in all the samples.

Fig. 8 shows the stress–strain curves of the SS, aged and FSP samples. The mechanical properties of the samples are given in Table 2. The 7055–0.25Sc sample exhibited higher strength than the 7055 sample under the same treatment conditions. Both the strengths and ductilities of the two SS samples were enhanced by

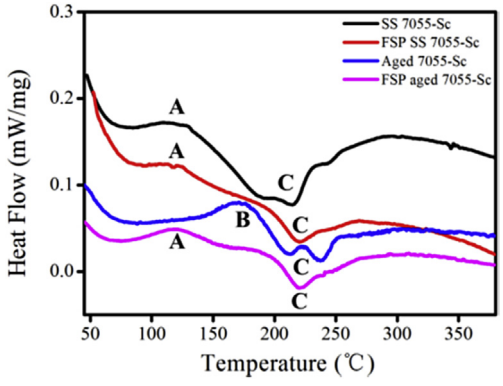

Fig. 7. DSC curves for 7055–0.25Sc samples under various conditions.

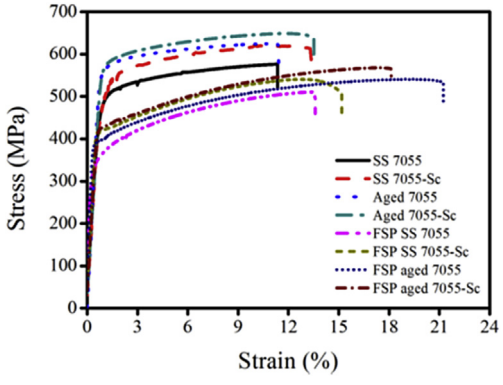

Fig. 8. Stress–strain curves for 7055 and 7055–0.25Sc samples under various conditions.

Table 2
Tensile properties of 7055 and 7055–0.25Sc samples under various conditions (YS: yield strength; UTS: ultimate tensile strength; EL: tensile elongation).

		YS (MPa)	UTS (MPa)	EL (%)
SS	7055	467 ± 5	576 ± 6	11 ± 1.2
	7055–0.25Sc	470 ± 4	620 ± 4	13 ± 1.5
Aged	7055	562 ± 3	620 ± 2	11 ± 0.8
	7055–0.25Sc	567 ± 3	649 ± 3	14 ± 0.5
FSP SS	7055	337 ± 3	510 ± 3	13 ± 0.2
	7055–0.25Sc	436 ± 3	560 ± 4	15 ± 0.3
FSP aged	7055	388 ± 1	541 ± 3	21 ± 0.7
	7055–0.25Sc	438 ± 2	578 ± 3	18 ± 0.6

aging. After FSP, the strengths of the SS and aged samples decreased, but the ductilities of them increased. Pre-aging enhanced both the strengths and ductilities of the FSP samples. Of the FSP samples, the FSP aged 7055–0.25Sc sample exhibited the highest strength, with the UTS reaching 578 MPa, which was even higher than that of the SS 7055 sample. The FSP aged 7055 sample exhibited better ductility than the other samples, and the EL of this sample reached as high as 21%.

The fracture surfaces of the aged and FSP aged samples are shown in Fig. 9. Compared with those of the aged samples, the fracture surfaces of the FSP sample exhibited finer and more homogenous dimples. Sc addition also refined the dimples of the aged and FSP samples.

4. Discussion

FSP improved the ductility of the 7055 and 7055–0.25Sc alloys (Fig. 8). Compared with the base metals (BMs), the FSP samples exhibited finer and more homogenous dimples after tensile testing (Fig. 9). This means that strain localization could be prevented by redistribution of the stresses in the FSP samples during tension [40].

Although the GB strengthening of the 7055 and 7055–0.25Sc alloys was enhanced by FSP due to FSP-induced grain refinement (Figs. 2a and 4a), the decreases in solid solution strengthening led to a decrease in the strength of the samples after FSP (Fig. 8). In previous studies, low heat input technology, which can inhibit the coarsening of the recrystallized grains and the precipitated phase of Al alloys during FSP, was widely used to enhance the strength of the FSP Al alloys [4,7,20,31]. In the present study, it was found that Sc addition and pre-aging could also affect the grain size and precipitation process of the FSP Al alloys (Figs. 4–7), and thus could optimize the mechanical properties of the FSP Al alloys.

4.1. Sc addition

The numerous $Al_3(Sc,Zr)$ particles in the 7055–0.25Sc samples (Fig. 3c and d) can strongly pin the GBs and dislocations during FSP, and thereby prevent intense grain growth. Compared with the FSP 7055 samples, the FSP 7055–0.25Sc samples therefore exhibit finer grains under the same conditions.

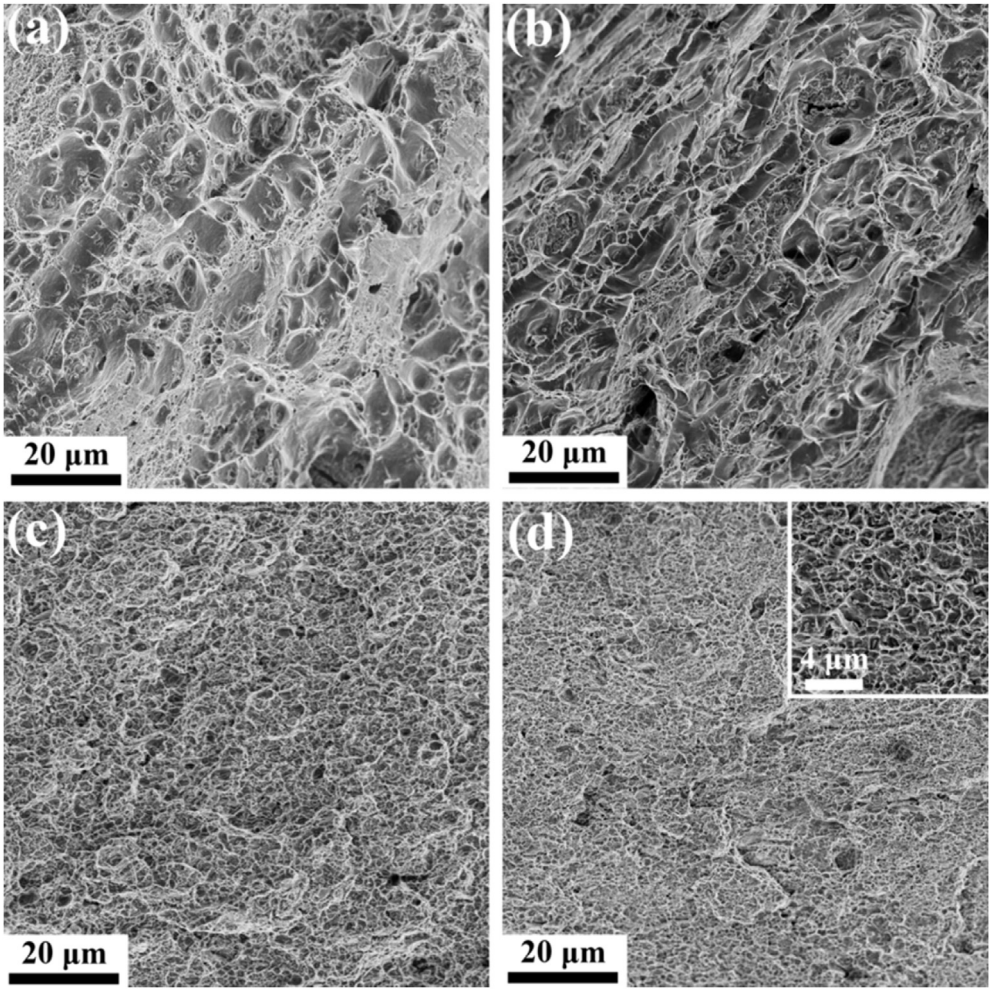

Fig. 9. Fracture surfaces of aged (a) 7055 and (b) 7055–0.25Sc samples, and FSP aged (c) 7055 and (d) 7055–0.25Sc samples.

The η phase precipitated on the Al_3Zr and $Al_3(Sc,Zr)$ particles in the FSP samples (Fig. 6a and c). This means that the Al_3Zr or $Al_3(Sc,Zr)$ particles in the 7055 and 7055–0.25Sc alloys provided preferential nucleation sites for the precipitates during FSP. The density of the $Al_3(Sc,Zr)$ phase in the 7055–0.25Sc alloy was significantly higher than that of Al_3Zr in the 7055 alloy (Fig. 2a and c). Greater numbers of preferential nucleation sites in the 7055–0.25Sc alloy led to a higher precipitation efficiency being obtained in this alloy during FSP, and the FSP 7055–0.25Sc sample therefore exhibits a finer and higher density η phase (Fig. 6a and c).

Due to the finer grains, the higher density of precipitated phases (including the $Al_3Zr/Al_3(Sc,Zr)$, η′ and η phases), and the finer η phase, the FSP 7055–0.25Sc samples exhibited higher strength than the FSP 7055 samples under the same conditions (Fig. 8).

4.2. Pre-aging

The absence of peak B in the DSC curves for the SS and FSP samples means that these samples did not contain the η′ phase (Fig. 7). During FSP, the aged 7055 and 7055–0.25Sc samples undergo deformation at elevated temperatures, resulting in a change of part of the η′ phase into the η phase. However, the density of the η phase in the FSP aged samples was significantly lower than that in the FSP SS samples (Fig. 6), and the FSP aged samples exhibited a higher intensity of the GP zones dissolution peak (peak A) than the FSP SS samples (Fig. 7). Based on the above phenomena, it can be inferred that some of the η′ phase in the aged samples dissolved into the Al matrix during FSP. Thus, the precipitation process of the samples during FSP was affected by the pre-aging, and the quantity of the solute atoms in the FSP aged samples was higher than that in the FSP SS samples.

The pre-aging also led to grain coarsening in the FSP samples (Fig. 4). The phenomenon that BM temper affected the grain size of the FSP or FSW samples was also observed in other 7xxx Al alloys [21,25]. The η phase precipitated along the GBs [13–15, 41], and the coarsening of grains was inhibited by the η phase due to the GB pinning effect of this phase [21]. Thus, coarser recrystallization grains were observed in the FSP aged samples due to the lower density of the η phase (Fig. 6).

The strength of the FSP samples was enhanced by pre-aging (Fig. 8). Compared with the FSP SS samples, the FSP aged samples exhibited higher solid solution strengthening due to the dissolution of the η′ precipitates into the Al lattice during FSP. The combination of high GB strengthening, precipitation strengthening, and solid solution strengthening therefore led to the FSP aged 7055–0.25Sc sample exhibiting the highest strength of the FSP samples.

Compared with the FSP SS samples, the FSP aged samples also exhibited higher ductility (Fig. 8). This can be mainly attributed to the low density of the η phase (Fig. 6) and the coarse equiaxed grain structure (Fig. 4). Firstly, the low density of the η phase in the FSP aged samples decreased the number of crack nucleation sites and preferential crack propagation paths during the tensile test. Thus, the FSP aged samples achieved considerable elongation before failure. Secondly, the UFG Al alloys always exhibit low dislocation storage capacity, which can reduce the work hardening capacity and ductility of alloys [1]. The FSP aged samples exhibited larger grain sizes than the FSP SS samples, and more dislocations could accumulate inside the grain interior during deformation. The work hardening capacity and ductility of the FSP samples were therefore improved by the pre-aging.

5. Conclusions

In this study, the effects of minor Sc addition and pre-aging on the microstructure and mechanical properties of FSP 7055 Al alloy were studied. The following conclusions can be reached:

(1) The addition of Sc led to the formation of the $Al_3(Sc,Zr)$ phase, which can pin GBs and provide more nucleation sites for the η precipitate phase in the 7055 alloy during FSP. Thus, Sc addition can effectively inhibit grain coarsening in recrystallization, refine the η phase, and increase the density of the η phase in the FSP 7055 alloy.

(2) Dissolution of the η′ phase during FSP led the FSP 7055 and 7055–0.25Sc alloys with pre-aging to exhibit a lower η phase density than the FSP samples without pre-aging. Pre-aging also led to the coarsening of grains in the FSP samples due to the weakened GB pinning effect from the reduced density of the η phase.

(3) The room-temperature mechanical properties of the FSP 7055 alloy were improved by the addition of Sc and pre-aging. Due to the high GB strengthening, precipitation strengthening, and solid solution strengthening, the FSP aged 7055-Sc alloy showed the highest ultimate tensile strength of 578 MPa, while the low density of the η phase and the coarse equiaxed grain structure led the aged 7055 Al alloy after FSP to show the largest elongation of 21%.

Acknowledgements

This work was funded by the National Natural Science Foundation of China (No. 51601045), the Guangxi “Bagui” Teams for Innovation and Research, Research Program of Science and Technology of Guangxi (No. GKAB16380021), and Guangxi Natural Science Foundation (No. 2016GXNSFDA380028).

References

[1] Y.T. Zhu, X.Z. Liao, Nanostructured metals: retaining ductility, Nat. Mater. 3 (2004) 351–352.
[2] I. Charit, R.S. Mishra, Low temperature superplasticity in a friction-stir-processed ultrafine grained Al–Zn–Mg–Sc alloy, Acta Mater. 53 (2005) 4211–4223.
[3] Y.H. Zhao, X.Z. Liao, S. Cheng, E. Ma, Y.T. Zhu, Simultaneously increasing the ductility and strength of nanostructured alloys, Adv. Mater. 18 (2006) 2280–2283.
[4] Z.Y. Ma, Friction stir processing technology: a review, Metall. Mater. Trans. A 39 (2008) 642–658.
[5] F. Zarghani, S.M. Mousavizade, H.R. Ezatpour, G.R. Ebrahimi, High mechanical performance of similar Al joints produced by a novel spot friction welding technique, Vacuum 147 (2018) 172–186.
[6] R.S. Mishra, Z.Y. Ma, Friction stir welding and processing, Mater. Sci. Eng. R 50 (2005) 1–78.
[7] Z.Y. Ma, R.S. Mishra, Development of ultrafine-grained microstructure and low temperature (0.48 Tm) superplasticity in friction stir processed Al–Mg–Zr, Scr. Mater. 53 (2005) 75–80.
[8] F.C. Liu, Z.Y. Ma, F.C. Zhang, High strain rate superplasticity in a micro-grained Al–Mg–Sc alloy with predominant high angle grain boundaries, J. Mater. Sci. Technol. 28 (2012) 1025–1030.
[9] F.C. Liu, Z.Y. Ma, Contribution of grain boundary sliding in low-temperature superplasticity of ultrafine-grained aluminum alloys, Scr. Mater. 62 (2010) 125–128.
[10] P. Liu, Y. Li, G.M. Zhang, K.Y. Feng, Relation between thermal effect and phase transformation of aluminium matrix surface composite adding Al-based amorphous fabricated by FSP, Vacuum 131 (2016) 65–68.
[11] J.R. Zuo, L.G. Hou, J.T. Shi, H. Cui, L.Z. Zhuang, J.S. Zhang, Enhanced plasticity and corrosion resistance of high strength Al–Zn–Mg–Cu alloy processed by an improved thermomechanical processing, J. Alloy. Comp. 716 (2017) 220–230.
[12] L.L. Wei, Q.L. Pan, H.F. Huang, L. Feng, Y.L. Wang, Influence of grain structure and crystallographic orientation on fatiguecrack propagation behavior of 7050 alloy thick plate, Int. J. Fatig. 66 (2014) 55–64.
[13] D. Wang, D.R. Ni, Z.Y. Ma, Effect of pre-strain and two-step aging on microstructure and stress corrosion cracking of 7050 alloy, Mater. Sci. Eng. A 494 (2008) 360–366.
[14] D. Wang, Z.Y. Ma, Z.M. Gao, Effects of severe cold rolling on tensile properties and stress corrosion cracking of 7050 aluminum alloy, Mater. Chem. Phys. 117 (2009) 228–233.
[15] D. Wang, Z.Y. Ma, Effect of pre-strain on microstructure and stress corrosion cracking of over-aged 7050 aluminum alloy, J. Alloy. Comp. 469 (2009) 445–450.
[16] K. Wang, F.C. Liu, Z.Y. Ma, F.C. Zhang, Realization of exceptionally high elongation at high strain rate in a friction stir processed Al–Zn–Mg–Cu alloy with the presence of liquid phase, Scr. Mater. 64 (2011) 572–575.

[17] A. Orozco-Caballero, M. Álvarez-Leal, D. Verdera, P. Rey, O.A. Ruana, F. Carreño, Evaluation of the mechanical anisotropy and the deformation mechanism in a multi-pass friction stir processed Al–Zn–Mg–Cu alloy, Mater. Des. 125 (2017) 116–125.
[18] A. Orozco-Caballero, M. Álvarez-Leal, P. Hidalgo-Manrique, C.M. Cepeda-Jiménez, O.A. Ruano, F. Carreño, Grain size versus microstructural stability in the high strain rate superplastic response of a severely friction stir processed Al–Zn–Mg–Cu alloy, Mater. Sci. Eng. A 680 (2017) 329–337.
[19] A. Orozco-Caballero, P. Hidalgo-Manrique, C.M. Cepeda-Jiménez, P. Rey, D. Verdera, O.A. Ruano, F. Carreño, Strategy for severe friction stir processing to obtain acute grain refinement of an Al–Zn–Mg–Cu alloy in three initial precipitation states, Mater. Charact. 112 (2016) 197–205.
[20] F.C. Liu, Z.Y. Ma, Low-temperature superplasticity of friction stir processed Al–Zn–Mg–Cu alloy, Scr. Mater. 58 (2008) 667–670.
[21] Y. Chen, H. Ding, Z.H. Cai, J.W. Zhao, J.Z. Li, Effect of initial base metal temper on microstructure and mechanical properties of friction stir processed Al-7B04 alloy, Mater. Sci. Eng. A 650 (2016) 396–403.
[22] S.M. Bayazid, H. Farhangi, H. Asgharzadeh, L. Radan, A. Ghahramani, A. Mirhaji, Effect of cyclic solution treatment on microstructure and mechanical properties of friction stir welded 7075 Al alloy, Mater. Sci. Eng. A 649 (2016) 293–300.
[23] N. Martinez, N. Kumar, R.S. Mishra, K.J. Doherty, Effect of tool dimensions and parameters on the microstructure of friction stir welded aluminum 7449 alloy of various thicknesses, Mater. Sci. Eng. A 684 (2017) 470–479.
[24] F. Zhang, X.K. Su, Z.Y. Chen, Z.R. Nie, Effect of welding parameters on microstructure and mechanical properties of friction stir welded joints of a super high strength Al–Zn–Mg–Cu aluminum alloy, Mater. Des. 67 (2015) 483–491.
[25] C. Sharma, D.K. Dwivedi, P. Kumar, Fatigue behavior of friction stir weld joints of Al–Zn–Mg alloy AA7039 developed using base metal in different temper condition, Mater. Des. 64 (2014) 334–344.
[26] S.D. Ji, X.C. Meng, R.F. Huang, L. Ma, S.S. Gao, Microstructures and mechanical properties of 7N01-T4 aluminum alloy joints by active-passive filling friction stir repairing, Mater. Sci. Eng. A 664 (2016) 94–102.
[27] R.K.R. Singh, C. Sharma, D.K. Dwivedi, N.K. Mehta, P. Kumar, The microstructure and mechanical properties of friction stir welded Al–Zn–Mg alloy in as welded and heat treated conditions, Mater. Des. 32 (2011) 682–687.
[28] Q.Z. Wang, Z.X. Zhao, Y. Zhao, K. Yan, C. Liu, H. Zhang, The strengthening mechanism of spray forming Al–Zn–Mg–Cu alloy by underwater friction stir welding, Mater. Des. 102 (2016) 91–99.
[29] Y. Deng, B. Peng, G.F. Xu, Q.L. Pan, Z.M. Yin, R. Ye, Y.J. Wang, L.Y. Lu, Effects of Sc and Zr on mechanical property and microstructure of tungsten inert gas and friction stir welded aerospace high strength Al–Zn–Mg alloys, Mater. Sci. Eng. A 639 (2015) 500–513.
[30] Z. Zhang, B.L. Xiao, Z.Y. Ma, Enhancing mechanical properties of friction stir welded 2219Al-T6 joints at high welding speed through water cooling and post-welding artificial ageing, Mater. Charact. 106 (2015) 255–265.
[31] P. Xue, B.L. Xiao, Q. Zhang, Z.Y. Ma, Achieving friction stir welded pure copper joints with nearly equal strength to the parent metal via additional rapid cooling, Scr. Mater. 64 (2011) 1051–1054.
[32] F.J. Liu, Y. Ji, Q.S. Meng, Z.S. Li, Microstructure and corrosion resistance of laser cladding and friction stir processing hybrid modification Al-Si coatings on AZ31B, Vacuum 133 (2016) 31–37.
[33] H.J. Jiang, C.Y. Liu, B. Zhang, P. Xue, Z.Y. Ma, K. Luo, M.Z. Ma, R.P. Liu, Simultaneously improving mechanical properties and damping capacity of Al-Mg-Si alloy through friction stir processing, Mater. Charact. 131 (2017) 425–430.
[34] B. Li, Q.L. Pan, X. Huang, Z.M. Yin, Microstructures and properties of Al-Zn-Mg-Mn alloy with trace amounts of Sc and Zr, Mater. Sci. Eng. A 616 (2014) 219–228.
[35] M. Zhang, T. Liu, C.N. He, J. Ding, E.Z. Liu, C.S. Shi, J.J. Li, N.Q. Zhao, Evolution of microstructure and properties of Al–Zn–Mg–Cu–Sc–Zr alloy during aging treatment, J. Alloy. Comp. 658 (2016) 946–951.
[36] W.B. Zhou, C.Y. Liu, P.F. Yu, B. Zhang, Z.Y. Ma, K. Luo, M.Z. Ma, R.P. Liu, Effect of scandium on microstructure and mechanical properties of high zinc concentration aluminum alloys, Mater. Charact. 127 (2017) 371–378.
[37] C.Y. Liu, X. Zhang, C.Q. Xia, Z.H. Feng, S.G. Liu, Z.G. Zhang, M.Z. Ma, R.P. Liu, Effects of Sc addition and rolling on the microstructure and mechanical properties of Al–35Zn alloys, Mater. Sci. Eng. A 703 (2017) 45–53.
[38] S.D. Liu, X.M. Zhang, M.A. Chen, J.H. You, Influence of aging on quench sensitivity effect of 7055 aluminum alloy, Mater. Charact. 59 (2008) 53–60.
[39] H.L. Zhu, A.K. Dahle, A.K. Ghosh, Microstructure formation in AlSi4MgMn and AlMg5Si2Mn high-pressure die castings, Metall. Mater. Trans. A 40 (2009) 598–608.
[40] D. Yadav, R. Bauri, Effect of friction stir processing on microstructure and mechanical properties of aluminium, Mater. Sci. Eng. A 539 (2012) 85–92.
[41] Y.Q. Xu, L.H. Zhan, S.J. Li, X.T. Wu, Effect of stress-aging treatments on precipitates of pre-retrogressed Al–Zn–Mg–Cu alloy, Rare Metal Mater. Eng. 46 (2017) 355–362.